

# A versatile electronic hole in one-electron oxidized Ni<sup>II</sup> bis-salicylidene phenylenediamine complexes†

Olaf Rotthaus,<sup>a</sup> Olivier Jarjayes,<sup>\*a</sup> Carlos Perez Del Valle,<sup>b</sup> Christian Philouze<sup>a</sup> and Fabrice Thomas<sup>\*a</sup>

Received (in Cambridge, UK) 2nd July 2007, Accepted 1st August 2007

First published as an Advance Article on the web 28th August 2007

DOI: 10.1039/b710027b

The nickel complexes  $1^{+}$ – $3^{+}$  exhibit a delocalized radical character, the extent of which depends on the electronic properties of the phenolate *para*-substituent.

Phenoxy radicals coordinated to divalent or trivalent metal ions are the focus of considerable interest since the discovery of a Cu<sup>II</sup>-tyrosyl radical entity in the active site of galactose oxidase.<sup>1</sup> Several Cu<sup>II</sup>-coordinated phenoxy radicals have been characterized during the last decade in order to mimic the enzyme active site.<sup>2</sup> Recently, nickel complexes of pro-radical,<sup>3</sup> and more specifically pro-phenoxy,<sup>4–7</sup> ligands (the phenolate moiety is substituted by electron-donating groups) have emerged in the literature. Compared to Cu<sup>II</sup>-phenoxy complexes, they exhibit ligand and metal redox active orbitals that are closer in energy. Consequently, either Ni<sup>II</sup>-phenoxy or Ni<sup>III</sup>-phenolate redox state are expected to be reached upon one-electron oxidation, making these compounds particularly interesting. A more striking feature has been recently reported for some nickel-salen complexes in non coordinating solvents: The ligand SOMO is found to be delocalized over the metal, affording a “delocalized radical”.<sup>5–7</sup> We present herein a series of nickel-radical salen complexes  $1^{+}$ – $3^{+}$  that exhibit this delocalized radical character. For the first time we show that the degree of delocalization could be modulated by the electron-donating properties of phenolate *para*-substituent R (Fig. 1). In addition, we found that it greatly influences the affinity of exogenous ligands for the metal, and thus the ability of the complexes to exhibit valence tautomerism properties (tetracoordinated Ni<sup>I</sup>-phenoxy  $\leftrightarrow$  octahedral Ni<sup>III</sup>-phenolate

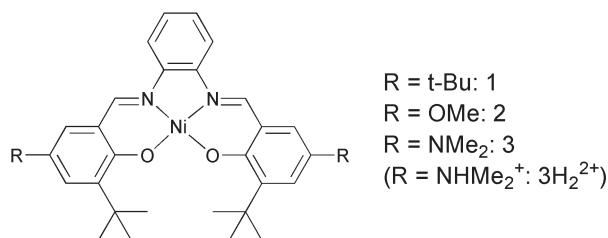


Fig. 1 Complexes used in this study.

<sup>a</sup>Département de Chimie Moléculaire - Chimie Inorganique Redox Biomimétique (CIRE) - UMR CNRS 5250, Université J. Fourier, B. P. 53, 38041 Grenoble cedex 9, France.

E-mail: Fabrice.Thomas@ujf-grenoble.fr; Fax: +33 476 514 846;

Tel: +33 476 514 373

<sup>b</sup>Département de Chimie Moléculaire - Chimie Théorique - UMR CNRS 5250, Université J. Fourier, B. P. 53, 38041 Grenoble cedex 9, France

† Electronic supplementary information (ESI) available: synthetic procedures, cyclic voltammetry curves, UV-Vis and EPR spectra, calculated SOMO. See DOI: 10.1039/b710027b

transformation). The tautomerism being accompanied by a thermochromism, such compounds are of growing interest in the development of molecular memories and switches.<sup>8</sup>

**1** has been previously reported,<sup>5</sup> while the low spin Ni<sup>II</sup> complexes **2** and **3H<sub>2</sub><sup>2+</sup>** were obtained by *in situ* synthesis. ‡ **3H<sub>2</sub><sup>2+</sup>** was deprotonated into **3** *in situ* by adding NEt<sub>3</sub>. The X-Ray crystal structures of **1**<sup>5</sup> and **3H<sub>2</sub><sup>2+</sup>**† shows a square planar geometry around the nickel atom that confirms its low spin nature. The UV-Vis spectra of **1**, **2** and **3** (Fig. 2a) exhibit intense absorption bands at 494 (10 500 M<sup>-1</sup> cm<sup>-1</sup>), 517 (9970 M<sup>-1</sup> cm<sup>-1</sup>) and 542 nm (8050 M<sup>-1</sup> cm<sup>-1</sup>) respectively that correspond to CT transitions.<sup>9</sup> As expected, the more electron-donating NMe<sub>2</sub> substituent gives rise to the longest wavelength absorption.

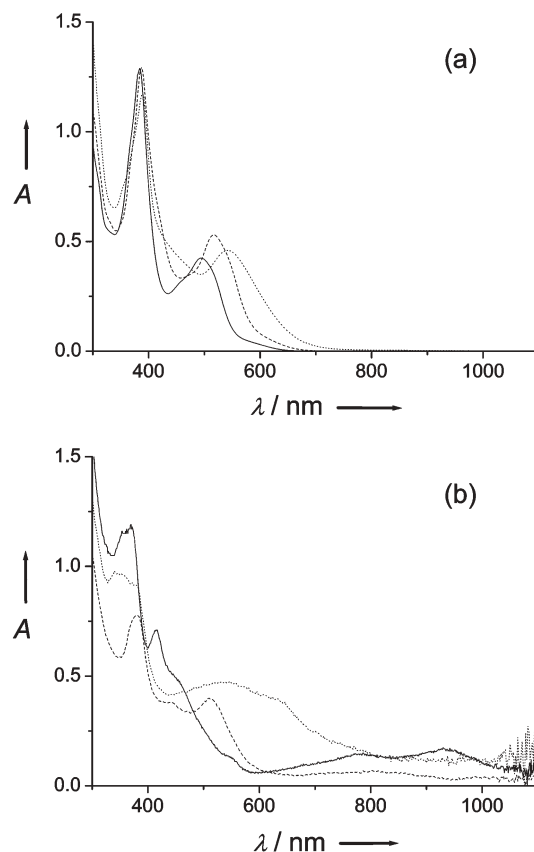


Fig. 2 Electronic spectra of CH<sub>2</sub>Cl<sub>2</sub> solutions of: (a) **1** ( $4 \times 10^{-5}$  M, solid lines), **2** ( $5.3 \times 10^{-5}$  M, dashed lines) and **3** ( $5.7 \times 10^{-5}$  M, dotted lines) at 298 K. (b) The electrogenerated **1**<sup>+</sup> ( $5 \times 10^{-5}$  M, solid lines), **2**<sup>+</sup> ( $3.3 \times 10^{-5}$  M, dashed lines) and **3**<sup>+</sup> ( $5 \times 10^{-5}$  M, dotted lines) at 233 K. The electrolytic solutions contain 0.005 M TBAP. *l* = 1.000 cm.

The cyclic voltammetry curves of **1** and **3** are characterized by two reversible one-electron-redox waves at  $E_{1/2}^1 = 582$  mV,  $E_{1/2}^1 = 802$  mV, and  $E_{1/2}^1 = -144$  mV,  $E_{1/2}^2 = 3$  mV (vs. Fc/Fc<sup>+</sup>) respectively, while a single one-electron oxidation wave is observed at  $E_{1/2}^1 = 356$  mV for **2**.<sup>10</sup> The shift in  $E_{1/2}^1$  according to the electronic properties of the phenolate *para*-substituent suggests a participation of the ligand in the oxidation locus.

The one-electron oxidized species **1**<sup>+</sup>, **2**<sup>+</sup> and **3**<sup>+</sup> were generated electrochemically in CH<sub>2</sub>Cl<sub>2</sub> containing 0.1 M TBAP as supporting electrolyte. The UV-Vis spectra of the corresponding cations **1**<sup>+</sup>, **2**<sup>+</sup> and **3**<sup>+</sup> (Fig. 2b) are characterized by intense transitions in the whole spectrum.<sup>9</sup> The bands observed in the NIR region are attributed to intervalence CT transitions,<sup>7</sup> while those in the 400–650 nm region may correspond to a combination of  $\pi$ - $\pi^*$  transitions of phenoxyl radicals<sup>11</sup> and phenolate-Ni CT transitions.

The 233 K EPR spectrum of **1**<sup>+</sup> in CH<sub>2</sub>Cl<sub>2</sub> (Fig. 3) is characterized by an isotropic signal at a  $g_{\text{iso}}$  value of 2.034, *i.e.* value intermediate between that of the phenoxyl radical complex of the zinc analogue of **1**, namely **1**<sub>Zn</sub><sup>+</sup>,<sup>12</sup> and those of Ni<sup>III</sup> complexes.<sup>13</sup> **1**<sup>+</sup> has thus a radical character with partial delocalization onto the orbital of the nickel ion. At 100 K in anhydrous CH<sub>2</sub>Cl<sub>2</sub> the EPR spectrum consists of a rhombic signal at  $g_1 = 2.06$  (broad),  $g_2 = 2.014$ ,  $g_3 = 1.991$  (see ESI<sup>†</sup>)<sup>14</sup> that again argues in favour of a delocalized radical with a contribution from the nickel orbital. This assumption is confirmed by DFT calculations at the B3LYP level (Fig. 4), showing a 6.6% Mulliken contribution of a nickel orbital (mainly  $d_{yz}$ ) to the total spin density. In addition, the ligand SOMO (Fig. 4) is found to be equally developed on both phenoxyl moieties pointing out stabilization of the radical by resonance.

In the presence of two molar equivalents of pyridine the 100 K EPR spectrum dramatically changes and becomes typical for a Ni<sup>III</sup> ion, with hyperfine coupling in each of the three  $g$ -components ( $g_{xx} = 2.200$ ,  $g_{yy} = 2.168$ ,  $g_{zz} = 2.027$ ,  $A_{xx} = A_{yy} = 1.65$  mT,  $A_{zz} = 2.14$  mT).<sup>5</sup> The well-resolved quintuplet in the high field component is the signature of a six-coordinate Ni<sup>III</sup> adduct **1**<sub>Py</sub><sup>+</sup> with two pyridines axially bonded. Upon pyridine ligation, the metal geometry is converted from square planar to octahedral, thus changing the energy of the nickel orbitals. As has been recently suggested,<sup>5,7</sup> an intramolecular electron transfer (valence tautomerism) occurs, shifting the electronic hole from the ligand to the metal.

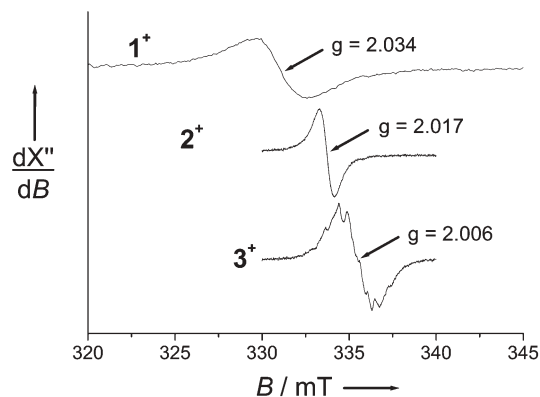


**Fig. 3** X-Band EPR spectra of CH<sub>2</sub>Cl<sub>2</sub> solutions (anhydrous + 0.1 M TBAP) of **1**<sup>+</sup> (1 mM), **2**<sup>+</sup> (0.5 mM) and **3**<sup>+</sup> (1 mM) at 233 K. Microwave Freq.: 9.42 GHz, power: 20 mW, Mod. Freq.: 100 KHz, Amp. 0.4 mT (**1**<sup>+</sup>), 0.05 mT (**2**<sup>+</sup>, **3**<sup>+</sup>).

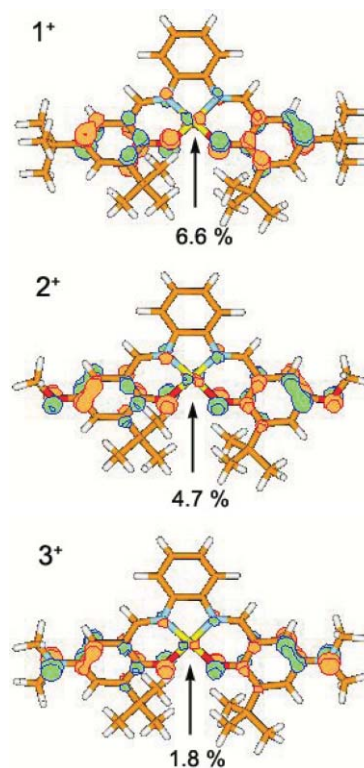


**Fig. 4** Optimized structures and calculated SOMO for **1**<sup>+</sup>, **2**<sup>+</sup> and **3**<sup>+</sup>; The Mulliken contribution of the nickel orbitals (mainly the  $d_{yz}$ ) to the total spin density is indicated.

The 233 K EPR spectrum of **2**<sup>+</sup> in CH<sub>2</sub>Cl<sub>2</sub> is dominated by an isotropic signal at  $g_{\text{iso}} = 2.017$  (Fig. 3). This  $g_{\text{iso}}$  value is again higher than that of **1**<sub>Zn</sub><sup>+</sup>, but significantly lower than that of **1**<sup>+</sup> and previously reported nickel-delocalized phenoxyl radicals.<sup>5–7</sup> In addition, the signal is much sharper than that of **1**<sup>+</sup>. **2**<sup>+</sup> is thus again a delocalized radical, but the contribution of nickel orbitals is less pronounced than in recently reported systems that are apparently similar. This fact is further confirmed by the nearly isotropic nature of the EPR signal at 100 K. In agreement with these findings, DFT calculations reveal that the nickel contribution to the total spin density is only 4.7% (Fig. 4), while a significant spin density is delocalized onto the methoxyl oxygen. Similarly to **1**<sup>+</sup>, the ligand SOMO of **2**<sup>+</sup> is equally developed on both phenoxyl moieties. Addition of pyridine to **2**<sup>+</sup> promotes valence tautomerism, as it does for **1**<sub>Py</sub><sup>+</sup>, affording the Ni<sup>III</sup> species **2**<sub>Py</sub><sup>+</sup>. The spin Hamiltonian parameters obtained from simulation of the EPR spectrum of **2**<sub>Py</sub><sup>+</sup> were found virtually similar to those of **1**<sub>Py</sub><sup>+</sup>: In the presence of pyridine, the nickel orbitals are thus poorly affected by the electronic properties of the phenolate *para*-substituent. In contrast, the affinity of pyridine for **2**<sup>+</sup> was found to be 30-times lower than for **1**<sup>+</sup> at 263 K.<sup>15</sup> This lower affinity is correlated to the degree of delocalization of the spin density on the metal. Pyridine is known to bind strongly to Ni<sup>III</sup> ions (its affinity for tetracoordinated Ni<sup>II</sup> ions is much lower), thus the weaker electronic hole on the nickel atom of **2**<sup>+</sup> (more marked Ni<sup>II</sup> character) lowers its affinity for pyridine.

The EPR spectrum of **3**<sup>+</sup> at 233 K was found to be dramatically different than those of **1**<sup>+</sup> and **2**<sup>+</sup>. **3**<sup>+</sup> exhibits an isotropic signal at  $g_{\text{iso}} = 2.006$  with hyperfine splitting (interaction of the electron spin

with NMe<sub>2</sub> nitrogen and hydrogen atoms). The  $g_{\text{iso}}$  value is very close to that reported for  $\text{I}_{\text{Zn}}^{+}$  showing that, among the series,  $\mathbf{3}^{+}$  has the strongest radical character. The very limited contribution of the nickel orbitals to the total spin density is also apparent from DFT calculations (Fig. 4). It is only 1.8% for  $\mathbf{3}^{+}$ , while a significant spin density is delocalized on the NMe<sub>2</sub> nitrogen. This delocalization could be also visualized through the planarity between the NMe<sub>2</sub> group and the phenoxyl ring. Addition of pyridine to  $\mathbf{3}^{+}$  in CH<sub>2</sub>Cl<sub>2</sub> results in a total loss of the EPR signal, suggesting that the pyridine adduct decomposes quickly. The chemical stability of the pyridine adduct thus appears correlated to the nature of the phenolate *para*-substituent. Increasing its electron-donating properties results in a lower chemical stability of the corresponding Ni<sup>III</sup> complexes.

In conclusion, in one-electron oxidized Ni<sup>II</sup> bis-salicylidene phenylenediamine complexes the electronic hole could be shifted by modifying the electronic properties of the phenolate *para*-substituent. The affinity of exogenous ligands for the complex, and thus its potentiality to exhibit valence tautomerism, is greatly influenced by the degree of delocalization.

## Notes and references

‡ Crystals were mounted on a Kappa CCD Nonius diffractometer equipped with graphite-monochromated Mo-K $\alpha$  radiation ( $\lambda = 0.71073 \text{ \AA}$ ) and a cryostream cooler. *Crystal data for*  $\mathbf{3H}_2^{2+} \cdot 2\text{Cl}^- \cdot 1.8\text{CHCl}_3 \cdot 1.2\text{H}_2\text{O}$ :  $\text{C}_{33.81}\text{H}_{43.81}\text{NiCl}_{7.43}\text{N}_4\text{O}_{3.25}$ ,  $M_w = 880.39$ , Red needle (0.41 × 0.37 × 0.25 mm), monoclinic, space group *P21/a*,  $a = 10.934(1)$ ,  $b = 20.635(2)$ ,  $c = 18.842(2) \text{ \AA}$ ,  $\alpha = 90$ ,  $\beta = 100.24(2)$ ,  $\gamma = 90^\circ$ ,  $V = 4183.3(7) \text{ \AA}^3$ ,  $Z = 4$ ,  $D_c = 1.398 \text{ g cm}^{-3}$ ,  $T = 293 \text{ K}$ ,  $\mu(\text{Mo-K}\alpha) = 0.975 \text{ mm}^{-1}$ . 58172 reflections were collected and corrected for Lorentz and polarization effects. Crystal structural solution (direct method) and refinement (by full-matrix least squares on  $F$ ) was performed using the teXsan analysis package. Non-hydrogen atoms were refined with anisotropic thermal parameters, while the other hydrogen atoms were generated on idealized positions, riding on the carrier atoms with isotropic thermal parameters. Of 9855 unique reflections ( $R_{\text{int}} = 0.0408$ ), 6177 were observed ( $F \geq 2.5\sigma(F)$ ) and used in the full-matrix least-squares refinement of 451 variables.  $R = 0.062$ ,  $R_w = 0.075$ , goodness of fit  $S = 1.94$ , max/min. residual peaks were  $1.86/-0.87 \text{ e. \AA}^{-3}$ . CCDC 649977. For crystallographic data in CIF or other electronic format see DOI: 10.1039/b710027b All calculations were performed using Gaussian 03 program<sup>16</sup> at the B3LYP level of theory and the LANL2DZ ECP basis set for Ni, C and H and LANL2DZdp ECP basis set for N and O.

- For reviews see: C. D. Borman, C. G. Sells, A. Sokolowski, M. B. Twitchett, C. Wright and A. G. Sykes, *Coord. Chem. Rev.*, 1999, **190–192**, 771; M. J. McPherson, M. R. Parsons, R. K. Spooner and C. M. Wilmot, *Handbook of metalloproteins*, John Wiley and Sons, Chichester, 2001, p. 1272; J. W. Whittaker, *Chem. Rev.*, 2003, **103**, 2347.
- For reviews see: B. A. Jazdzewski and W. B. Tolman, *Coord. Chem. Rev.*, 2000, **200–202**, 633; S. Itoh, M. Taki and S. Fukuzumi, *Coord. Chem. Rev.*, 2000, **198**, 3; P. Chaudhuri and K. Wieghardt, *Prog. Inorg. Chem.*, 2001, **50**, 151; P. Chaudhuri, K. Wieghardt, T. Weyhermüller, T. K. Paine, S. Mukherjee and C. Mukherjee, *Biol. Chem.*, 2005, **386**, 1023; F. Thomas, *Eur. J. Inorg. Chem.*, 2007, 2379.
- A. Aukauloo, X. Ottenwaelder, R. Ruiz, S. Poussereau, Y. Pei, Y. Journaux, P. Fleurat, F. Volatron, B. Cervera and M. C. Muñoz, *Eur. J. Inorg. Chem.*, 1999, 1067; D. Herebian, E. Bothe, E. Bill, T. Weyhermüller and K. Wieghardt, *J. Am. Chem. Soc.*, 2001, **123**, 10012; C.-H. Sieh, I.-J. Hsu, C.-H. Lee, S.-C. Ke, T. Wang, G.-H. Lee, Y. Wang, J.-M. Chen, J.-F. Lee and W. F. Lians, *Inorg. Chem.*, 2003, **42**, 3925; X. Ottenwaelder, R. Ruiz-Garcia, G. Blondin, R. Carasco, J. Cano, D. Lexa, Y. Journaux and A. Aukauloo, *Chem. Commun.*, 2004, 504; H. Ohtsu and K. Tanaka, *Angew. Chem., Int. Ed.*, 2004, **43**, 6301; S. Blanchard, F. Neese, E. Bothe, E. Bill, T. Weyhermüller and K. Wieghardt, *Inorg. Chem.*, 2005, **44**, 3636; H. Ohtsu and K. Tanaka, *Chem.–Eur. J.*, 2005, **11**, 3420.

- J. Müller, A. Kikuchi, E. Bill, T. Weyhermüller, P. Hildebrandt, L. Ould-Moussa and K. Wieghardt, *Inorg. Chim. Acta*, 2000, **297**, 265; Y. Shimazaki, S. Huth, S. Karasawa, S. Hirota, Y. Naruta and O. Yamauchi, *Inorg. Chem.*, 2004, **43**, 7816.
- O. Rotthaus, O. Jarjayes, F. Thomas, C. Philouze, C. Perez Del Vallee, E. Saint-Aman and J.-L. Pierre, *Chem.–Eur. J.*, 2006, **12**, 2293.
- Y. Shimazaki, F. Tani, K. Fului, Y. Naruta and O. Yamauchi, *J. Am. Chem. Soc.*, 2003, **125**, 10512; T. Glaser, M. Heidemeier, R. Fröhlich, P. Hildebrandt, E. Bothe and E. Bill, *Inorg. Chem.*, 2005, **44**, 5467; O. Rotthaus, F. Thomas, O. Jarjayes, C. Philouze, E. Saint-Aman and J.-L. Pierre, *Chem.–Eur. J.*, 2006, **12**, 6953; Y. Shimazaki, T. Yajima, F. Tani, S. Karasawa, K. Fukui, Y. Naruta and O. Yamauchi, *J. Am. Chem. Soc.*, 2007, **129**, 2559; L. Benisvy, R. Kannappan, Y.-F. Song, S. Mikkisyan, M. Huber, I. Mutikainen, U. Turpeinen, P. Gamez, L. Bernasconi, E. J. Baerends, F. S. Hartl and J. Reedijk, *Eur. J. Inorg. Chem.*, 2007, 631.
- T. Storr, E. C. Wasinger, R. C. Pratt and T. D. P. Stack, *Angew. Chem., Int. Ed.*, 2007, **46**, 5198.
- O. Kahn and C. J. Martinez, *Science*, 1998, **279**, 44.
- UV-Vis data ( $\lambda_{\text{max}}$  [nm] ( $\epsilon$  [ $\text{M}^{-1} \text{ cm}^{-1}$ ])): At 298 K for **1**: 384 (32 250), 494 (10 500); **2**: 387 (24 290), 517 (9970); **3**: 389 (20 580), 542 (8050). At 233 K for **1**<sup>+</sup>: 370 (21 700) 413 (12 200), 458 sh (7560), 780 br (2420), 936 br (2480); **2**<sup>+</sup>: 380 (23 600); 440 sh (11 540); 510 (12 110), 800 br (2030); **3**<sup>+</sup>: 346 (19 400); 380 sh (18 290); 548 br (9520), 630 (7890).
- The second oxidation peak is observed at  $E > 0.6 \text{ V}$  and corresponds to the transfer of more than two electrons. It has not been investigated further.
- J. G. Radziszewski, M. Gil, A. Gorski, J. Spanget-Larsen, J. Waluk and B. J. Mroz, *J. Chem. Phys.*, 2001, **115**, 9733.
- O. Rotthaus, O. Jarjayes, F. Thomas, C. Philouze, E. Saint-Aman and J.-L. Pierre, *Dalton Trans.*, 2007, **8**, 889.
- F. V. Lovecchio, E. S. Gore and D. H. Busch, *J. Am. Chem. Soc.*, 1974, **96**, 3109; H. J. Kruger and R. H. Holm, *Inorg. Chem.*, 1987, **26**, 3645; T. J. Collins, T. R. Nichols and E. S. Uffelman, *J. Am. Chem. Soc.*, 1991, **113**, 4708; F. Azevedo, M. A. Carrondo, B. Castro, M. Convery, D. Domingues, C. Freire, M. T. Duarte, K. Nielsen and I. C. Santos, *Inorg. Chim. Acta*, 1994, **219**, 43; D. Pinho, P. Gomes, C. Freire and B. De Castro, *Eur. J. Inorg. Chem.*, 2001, 1483.
- The EPR spectrum was found dependent on the conditions used to oxidize **1** into **1**<sup>+</sup>: Electrolysis at 233 K under Ar bubbling in freshly distilled standard CH<sub>2</sub>Cl<sub>2</sub> affords a species with an EPR signature typical for a Ni<sup>III</sup> ion. When the solvent is evaporated and the solid dissolved in fresh CH<sub>2</sub>Cl<sub>2</sub> a signature typical for a delocalized radical is obtained. A similar radical spectrum is observed when electrolysis is performed either at 298 K using anhydrous (>99.8%) CH<sub>2</sub>Cl<sub>2</sub> or in the more carbonated solvent C<sub>2</sub>H<sub>4</sub>Cl<sub>2</sub>, irrespective of the temperature. The discrepancy is attributed to the condensation of coordinating water molecules in CH<sub>2</sub>Cl<sub>2</sub> and/or the presence of impurities that bind axially at the solvent freezing point (the affinity of axial ligands strongly increases by decreasing the temperature, see ref 15). The affinity of axial ligands for **2**<sup>+</sup> being much weaker than for **1**<sup>+</sup>, its EPR spectra were found insensitive to the experimental conditions used to generate it.
- $K_{\text{py}}$  has been refined using the commercial SPECIFIT software for the equilibrium:  $\text{I}^+ + 2 \text{Py} \rightleftharpoons \text{I}_{\text{py}}^{2+}$ . The  $\log\beta$  values ( $\text{M}^{-2}$ ) as function of  $T$  are: For **1**<sup>+</sup>,  $6.71 \pm 0.09$  (298 K),  $7.94 \pm 0.14$  (263 K),  $8.76 \pm 0.18$  (243 K); For **2**<sup>+</sup>,  $6.44 \pm 0.15$  (263 K),  $7.46 \pm 0.12$  (236 K). The pyridine adducts **2**<sub>py</sub><sup>+</sup> at 298 K, and **3**<sub>py</sub><sup>+</sup> whatever is the temperature, were found too unstable to determine a  $\log\beta$  value.
- Gaussian 03, Revision C.02M. J. Frisch, G. W. Trucks, H. B. Schlegel, G. E. Scuseria, M. A. Robb, J. R. Cheeseman, J. A. Montgomery, Jr., T. Vreven, K. N. Kudin, J. C. Burant, J. M. Millam, S. S. Iyengar, J. Tomasi, V. Barone, B. Mennucci, M. Cossi, G. Scalmani, N. Rega, G. A. Petersson, H. Nakatsuji, M. Hada, M. Ehara, K. Toyota, R. Fukuda, J. Hasegawa, M. Ishida, T. Nakajima, Y. Honda, O. Kitao, H. Nakai, M. Klene, X. Li, J. E. Knox, H. P. Hratchian, J. B. Cross, V. Bakken, C. Adamo, J. Jaramillo, R. Gomperts, R. E. Stratmann, O. Yazyev, A. J. Austin, R. Cammi, C. Pomelli, J. W. Ochterski, P. Y. Ayala, K. Morokuma, G. A. Voth, P. Salvador, J. J. Dannenberg, V. G. Zakrzewski, S. Dapprich, A. D. Daniels, M. C. Strain, O. Farkas, D. K. Malick, A. D. Rabuck, K. Raghavachari, J. B. Foresman, J. V. Ortiz, Q. Cui, A. G. Baboul, S. Clifford, J. Cioslowski, B. B. Stefanov, G. Liu, A. Liashenko, P. Piskorz, I. Komaromi, R. L. Martin, D. J. Fox, T. Keith, M. A. Al-Laham, C. Y. Peng, A. Nanayakkara, M. Challacombe, P. M. W. Gill, B. Johnson, W. Chen, M. W. Wong, C. Gonzalez and J. A. Pople, Gaussian, Inc., Wallingford CT, 2004.